VETOR

Decentralized *versus* Centralized COVID-19 Interventions in Mozambique: A Metapopulation Modeling Study☆

Intervenções Descentralizadas *versus* Centralizadas da COVID-19 em Moçambique: Um Estudo de Modelagem Metapopulacional

Paulo Joaquim[1], Daisuke Takahash[2], Sansão A. Pedro[1†]

[1]*Eduardo Mondlane University, Faculty of Sciences, Maputo, Mozambique*
[2]*A. I. Systems Research Co., Ltd, Yoshidaushinomiya-cho, Sakyo-ku, Kyoto, Japan*
[†]**Corresponding author:** sansao.pedro@uem.ac.mz or sansaopedro@gmail.com

Abstract

Country-wide lockdowns often face resistance when perceived as overly broad or misaligned with local realities. Designing effective, context-sensitive interventions requires understanding whether centralized national or decentralized provincial measures are more appropriate. This study extends previous analyses by developing a stochastic metapopulation model to simulate COVID-19 transmission across Mozambique's 11 provinces during the first epidemic wave from March 22, 2020 to March 7, 2021. Human mobility was modeled via a radiation-based transition matrix, and the model was calibrated using effective population estimates and reported active cases. Three core intervention scenarios were evaluated including mobility without interventions, mobility with centralized national-triggered interventions, and mobility with decentralized province-specific triggers. Additional simulations assessed the robustness of interventions under varying physical distancing effectiveness ϵ, national thresholds νG, and provincial thresholds νL. Results indicate that decentralized interventions outperformed centralized approaches, delaying provincial epidemic peaks by 29 to 82 days, with a national average of 37 days, and reducing cumulative infections by $0.74-6.86\%$ across provinces, with a national reduction greater than 2.49%. Sensitivity analyses show that higher physical distancing effectiveness and stricter local thresholds further delay peaks, particularly in less-connected provinces. Global sensitivity analysis highlights transmission rate, interprovincial connectivity, and intervention efficacy as the most influential factors. These findings suggest that province-specific strategies provide a superior balance between epidemic control and socioeconomic resilience in resource-limited settings and demonstrate the importance of spatially explicit mobility-aware models to guide adaptive public health policies and future pandemic preparedness under heterogeneous regional conditions.

Keywords

COVID-19 • Mozambique • Decentralized interventions • Metapopulation modeling • Nonpharmaceutical interventions

Resumo

Confinamentos em todo o país frequentemente enfrentam resistência quando percebidos como excessivamente amplos ou desalinhados com as realidades locais. Conceber intervenções eficazes e sensíveis ao contexto exige compreender se as medidas centralizadas nacionais ou descentralizadas provinciais são mais adequadas. Este estudo amplia

☆This article is an extended version of the work presented at the XXVIII National Meeting on Computational Modeling (ENMC) & XVI Meeting on Science and Technology of Materials (ECTM), held in Montes Claros, Brazil, October 21–24, 2025.

análises anteriores ao desenvolver um modelo estocástico metapopulacional para simular a transmissão da COVID-19 nas 11 províncias de Moçambique durante a primeira onda epidémica, de 22 de março de 2020 a 7 de março de 2021. A mobilidade humana foi modelada através de uma matriz de transição baseada em radiação, e o modelo foi calibrado utilizando estimativas populacionais efetivas e casos ativos reportados. Foram avaliados três cenários centrais de intervenção: mobilidade sem intervenções, mobilidade com intervenções centralizadas acionadas por gatilhos nacionais, e mobilidade com intervenções descentralizadas acionadas por gatilhos específicos de cada província. Simulações adicionais avaliaram a robustez das intervenções sob diferentes valores da eficácia do distanciamento físico ϵ, do limiar nacional νG e do limiar provincial νL. Os resultados indicam que as intervenções descentralizadas superaram as abordagens centralizadas, atrasando os picos epidémicos provinciais em 29 a 82 dias, com uma média nacional de 37 dias, e reduzindo as infeções acumuladas em $0{,}74 - 6{,}86\%$ nas províncias, com uma redução nacional superior a 2,49%. Análises de sensibilidade mostram que maior eficácia do distanciamento físico e limiares locais mais restritivos atrasam ainda mais os picos, particularmente em províncias menos conectadas. A análise de sensibilidade global destaca a taxa de transmissão, a conectividade interprovincial e a eficácia da intervenção como os fatores mais influentes. Estes resultados sugerem que estratégias específicas por província proporcionam um equilíbrio superior entre controlo epidémico e resiliência socioeconómica em contextos com recursos limitados, e demonstram a importância de modelos espacialmente explícitos e sensíveis à mobilidade para orientar políticas de saúde pública adaptativas e o preparo para futuras pandemias em condições regionais heterogéneas.

Palavras-chave

COVID-19 • Moçambique • Intervenções descentralizadas • Modelagem metapopulacional • Intervenções não farmacêuticas

1 Introduction

The coronavirus disease 2019 (COVID-19), caused by the severe acute respiratory syndrome coronavirus 2 (SARS-CoV-2), triggered unprecedented global public health responses. To curb viral transmission during the early stages of the pandemic, many countries implemented nonpharmaceutical interventions (NPIs) including testing, isolation, contact tracing, quarantine, and movement restrictions [1, 2, 3]. In addition, governments adopted broad measures such as school and workplace closures, restrictions on public gatherings, and population mobility limitations [4, 5]. When timely and effectively applied, these interventions can reduce the effective reproduction number (R_e) below unity, thereby slowing transmission, limiting infections, reducing strain on healthcare systems, and lowering mortality [5, 6]. However, balancing epidemic control with socioeconomic stability remains a central challenge, especially in low- and middle-income countries where prolonged nationwide lockdowns can exacerbate economic inequality and social distress [7, 8].

In the context of Mozambique, the pandemic did not progress uniformly across the national territory. The first confirmed case was reported in Maputo City on March 22, 2020, and subsequent spread occurred to Maputo Province, Cabo Delgado, and eventually throughout the remaining provinces by mid-May 2020. By March 2023, the country had reported over 233,000 cumulative cases and more than 2,200 deaths [9, 10]. Authorities responded with a series of public health alerts and policy measures, including repeated States of Emergency and restrictions on economic and social activities. Despite these efforts, due to economic necessity and limited social protection mechanisms, compliance with some NPIs was uneven, particularly among populations dependent on informal employment [11, 12]. These socioeconomic realities underscore the complex trade-offs inherent in epidemic policymaking in contexts marked by vulnerability and informality.

The economic and social consequences of prolonged broad lockdowns can be severe. In Mozambique, estimates suggest that household poverty increased substantially, driving millions into deeper vulnerability, while national GDP growth contracted and employment declined [13, 14]. School closures, although necessary to limit transmission, adversely affected educational attainment, particularly in rural areas with limited connectivity and resources [15, 16]. These indirect costs highlight the need for more nuanced strategies that can balance epidemiological effectiveness with socioeconomic feasibility.

An emerging body of research suggests that regionally targeted and localized interventions can achieve more efficient epidemic control with lower social and economic disruption than blanket national policies. Empirical studies of localized lockdowns, such as those implemented in Chile, indicate that localized measures can slow transmission while imposing lower overall societal costs, though their effectiveness is modulated by spillover effects from neighboring regions [17]. Spatially explicit modeling approaches also show that regional heterogeneity and mobility patterns significantly shape epidemic trajectories, and that tailored interventions can improve outcomes relative to uniform strategies [18, 19]. In addition, data-driven metapopulation models from other settings (e.g., Belgium) demonstrate how social mixing and mobility reductions influence epidemic dynamics under phased exit strategies [20]. Furthermore, recent theoretical work emphasizes the importance of mobility and inter-regional travel in determining the effectiveness of local interventions and thresholds for action [21].

Despite these advances, there is a limited understanding of how centralized versus decentralized approaches perform in spatially heterogeneous environments such as Mozambique, where subnational variation in connectivity, population density, and socioeconomic conditions is pronounced. Existing metapopulation models that account for mobility and spatial structure provide a promising framework for evaluating such differential strategies [22, 23], but applications in low-resource settings remain scarce.

Given this gap, this study develops a stochastic metapopulation SEIAHRD model incorporating interprovincial mobility and heterogeneous contact patterns to evaluate the relative effectiveness of centralized (national) and decentralized (provincial) COVID-19 intervention strategies in Mozambique. The specific objectives are: (i) to compare the timing and magnitude of epidemic peaks under centralized and decentralized scenarios; (ii) to assess how intervention trigger thresholds influence epidemic dynamics; (iii) to quantify the role of contact reduction effectiveness in peak delay; and (iv) to identify key model parameters driving variability in epidemic timing via global sensitivity analysis. Through these analyses, we aim to provide evidence-based insights to inform adaptive, context-specific epidemic policy design in resource-limited and spatially heterogeneous settings.

2 Material and Methods

2.1 Metapopulation Epidemic Model

This study builds on the work of Joaquim et al. [24], who proposed a stochastic, discrete-time metapopulation epidemic model to simulate COVID-19 transmission in Mozambique. In that earlier model, the national territory was structured as a network of interconnected subpopulations, each corresponding to one of the eleven provinces of the country. In the present study, we extend that framework by modifying the force of infection to incorporate containment measures designed to distinguish between the impacts of centralized (national-level) and decentralized (province-level) intervention strategies. This extension was essential to evaluate how policy coordination (or its absence) influences the timing of epidemic peaks, the cumulative number of infections, and the overall burden on the health system, especially in a spatially heterogeneous and economically informal context such as Mozambique.

The model comprises 11 interacting subpopulations (provinces), with disease dynamics occurring independently within each province i, while interprovincial mobility allows the spatial spread of infection. The SEIAHRD model denotes a compartmental structure that divides individuals into seven disease-related states:**S** (susceptible), **E** (exposed), **I** (symptomatic infectious), **A** (asymptomatic infectious), **H** (hospitalized), **R** (recovered), and **D** (reported deaths). Each compartment reflects a key phase of disease progression and enables a more detailed representation of transmission patterns, health outcomes, and policy-relevant indicators such as hospitalization and death. The probability of infection is expressed by the force of infection $\lambda_i(t)$, defined as:

$$\lambda_i(t) = 1 - \left[1 - \beta_i \left(\xi + \frac{1-\xi}{N_i}\right)\right]^{N_i^+}, \tag{1}$$

where β_i is the infection rate, N_i denotes the total number of individuals in the subpopulation i, and $N_i^+ = I_i(t) + A_i(t) + H_i(t)$ represents the number of active cases. The parameter ξ regulates the type of incidence: for $\xi = 0$, the model follows the standard incidence; for $\xi = 1$, it follows density-dependent incidence, as discussed in Karatayev et al. [25].

Figure 1 illustrates the transition diagram of the SEIAHRD model in each node of the metapopulation network.

As the epidemic progresses, individuals move between subpopulations. For each compartment X ({S, E, I, A, R}) in subpopulation i and time t, after determining $X_{ij}(t)$, which represents the number of individuals traveling from i to j. $\sum_j X_{ij}(t)$ represents the total number of individuals in compartment X leaving subpopulation i for other subpopulations j. On the other hand, $\sum_j X_{ji}$ indicates the total number of individuals entering i from different subpopulations j. In each compartment X, an individual has the possibility to move from subpopulation i to one of $J = 10$ other subpopulations. So, incorporating interprovincial mobility terms, leading to the following metapopulation model for COVID-19 transmission, described by the system of Eq. (2).

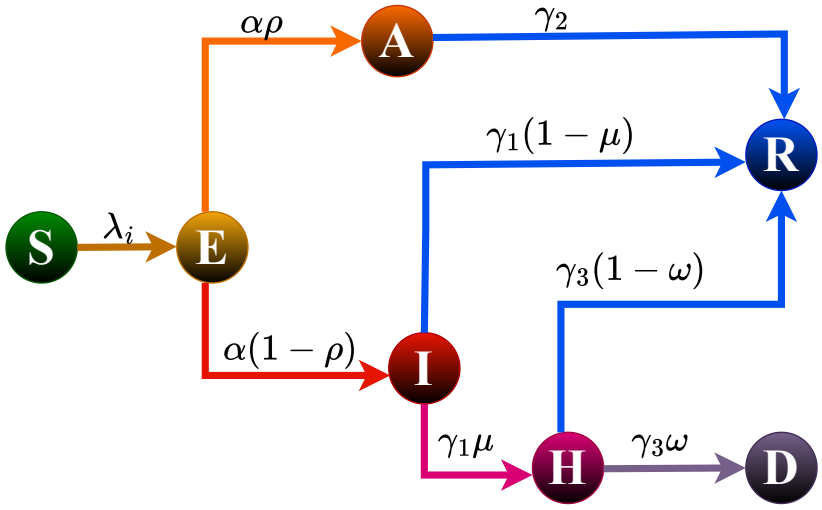

Figure 1: Transition diagram of the **SEIAHRD** epidemic model in each subpopulation.

$$
\begin{aligned}
S_i(t+h) &= S_i(t) - B_{12}(t) - \sum_j S_{ij}(t) + \sum_j S_{ji}(t) \\
E_i(t+h) &= E_i(t) + B_{12}(t) - B_{23}(t) - B_{24}(t) - \sum_j E_{ij}(t) + \sum_j E_{ji}(t) \\
I_i(t+h) &= I_i(t) + B_{23}(t) - B_{35}(t) - B_{36}(t) - \sum_j I_{ij}(t) + \sum_j I_{ji}(t) \\
A_i(t+h) &= A_i(t) + B_{24}(t) - B_{46}(t) - \sum_j A_{ij}(t) + \sum_j A_{ji}(t) \\
H_i(t+h) &= H_i(t) + B_{35}(t) - B_{56}(t) - B_{57}(t) \\
R_i(t+h) &= R_i(t) + B_{36}(t) + B_{46}(t) + B_{56}(t) - \sum_j R_{ij}(t) + \sum_j R_{ji}(t) \\
D_i(t+h) &= D_i(t) + B_{57}(t),
\end{aligned}
\tag{2}
$$

where

$$
\begin{aligned}
&B_{12}(t) \sim \text{Bin}(S_i(t), P_{12}(t)), B_{23}(t) \sim \text{Bin}(E_i(t), P_{23}(t)), && B_{24}(t) \sim \text{Bin}(E_i(t), P_{24}(t)), \\
&B_{35}(t) \sim \text{Bin}(I_i(t), P_{35}(t)), B_{36}(t) \sim \text{Bin}(I_i(t), P_{36}(t)), && B_{46}(t) \sim \text{Bin}(A_i(t), P_{46}(t)), \\
&B_{56}(t) \sim \text{Bin}(H_i(t), P_{56}(t)), B_{57}(t) \sim \text{Bin}(H_i(t), P_{57}(t)).
\end{aligned}
$$

The random variables above involve binomial distributions $\text{B}(n, p)$ with the following transition probabilities: $P_{12}(t) = \lambda_i(t)$, where $\lambda_i(t)$ is the force of infection; $P_{23} = \alpha(1-\rho)$, with α as the incubation rate and $(1-\rho)$ the proportion of symptomatic cases; $P_{24} = \alpha\rho$, where ρ is the proportion of asymptomatic cases; $P_{35} = \gamma_1\mu$, with γ_1 as the recovery rate and μ the proportion hospitalized; $P_{36} = \gamma_1(1-\mu)$; $P_{46} = \gamma_2$, the recovery rate for asymptomatic cases; $P_{56} = \gamma_3(1-\omega)$, where γ_3 is the recovery rate for hospitalized cases and $1-\omega$ the proportion recovered; $P_{57} = \gamma_3\omega$, with ω as the mortality rate post-hospitalization.

For a more detailed description of the base epidemic model, the interprovincial mobility dynamics, and the formulation of the resulting metapopulation model from the coupling of these components, we refer the reader to the methodological sections presented in previous works [23, 24].

2.2 Intervention Measures

To incorporate containment measures into the numerical model, we considered the closure and subsequent reopening of schools and workplaces. This dynamic was modeled using the function $C_i(t)$, which defines the activation of interventions based on time and case thresholds:

$$C_i(t) = \begin{cases} 1 & \text{if } t_{n=1} < t < t_{\text{initial}}, \\ 1 & \text{if } t > t_{\text{initial}} + t_{n=1} \text{ and } (N_G^+ > \nu G \text{ or } t < t_G + \delta_C), \\ 1 & \text{if } t > t_{\text{initial}} + t_{n=1} \text{ and } (N_i^+ > \nu L \text{ or } t < t_{L,i} + \delta_C), \\ 0 & \text{otherwise.} \end{cases} \tag{3}$$

In this function, presented in Eq. (3), $t_{n=1}$ represents the period when the country had $n = 1$ active case; t_{initial} is the period of the first school closure; N_G^+ and N_i^+ denote the national and local numbers of active cases, respectively; νG and νL are the thresholds for national and provincial closure; t_G and $t_{L,i}$ correspond to the dates of the last national and local decrees, respectively; and $\delta_C = 30$ represents the minimum closure duration.

This function is then integrated into the modeling of the fraction of contacts remaining after the implementation of the interventions, represented by:

$$F_i(t) = w[1 - \epsilon C_i(t)] + (1 - w), \tag{4}$$

where w is the weight assigned to contact reduction in formal settings (schools and workplaces), and ϵ denotes the effectiveness of the implemented measures.

By introducing $F_i(t)$ into the infection force equation, we obtain:

$$\lambda_i(t) = 1 - \left[1 - F_i(t)\beta_i \left(\xi + \frac{1-\xi}{N_i}\right)\right]^{N_i^+}, \tag{5}$$

which captures the direct impact of non-pharmaceutical interventions on the transmission dynamics.

To evaluate the impact of policy coordination, two main intervention strategies were analyzed. In the centralized strategy, containment measures were triggered based on national epidemiological thresholds, leading to simultaneous interventions across all provinces. In contrast, in the decentralized strategy, interventions were implemented independently by provincial authorities based on local case thresholds. This comparison allows us to quantify how policy synchronization affects epidemic timing, spatial spread, and peak healthcare demand.

2.3 Model Parameters and Sensitivity Analysis

The parameter values used in the simulation of intervention measures are shown in Table 1 and Table 2.

Table 1: Additional parameter values for simulations with global intervention measures.

Parameter	Definition	Value	Source	Province
w	Proportion of contacts in schools and workplaces	0.32	[26, 27, 28]	All
ϵ	Effectiveness of physical distancing	0.64	[25]	
δ_C	Minimum closure duration period	30	[29]	
νG	Threshold to close the country	3249	[30]	

Detailed information on the data, calibration procedures, and the other parameter values is available in our previous study [24], where these processes are thoroughly described.

The robustness of the model inferences was assessed through a global sensitivity analysis based on Sobol indices (first-order and total), with the time of the infection peak ($T_{\text{peak},i}$) in each province as the quantity of interest. This quantity is particularly relevant from a public health perspective, as delaying the epidemic peak is directly associated with the health system's preparedness capacity and the effectiveness of non-pharmaceutical interventions [31, 32].

First-order Sobol indices (S_i) measure the direct contribution of each parameter to the output variance, while total indices (S_{T_i}) also incorporate all interactions of that parameter with others [33, 34]. The difference $S_{T_i} - S_i$ indicates the fraction of variance due exclusively to interactions involving parameter i.

To quantify uncertainty, we considered the transmission rate β_i, the incidence control parameter ξ, the proportion of contacts in schools and workplaces w, and the effectiveness of physical distancing measures ϵ. For this process, we first defined a range of $[-30\%, +30\%]$ for each of the aforementioned parameters. Next, we generated a sample matrix combining parameter values within this range using the `.sample_sobol()` function, based on the work of Sobol [35] and implemented in the Python SALib library developed by Herman and Usher [36]. Using the sample of parameter value combinations, we instantiated and ran the epidemiological submodels corresponding to

Table 2: Additional parameter values for simulations in Scenario 2.

Parameter	Definition	Value	Source	Province
w	Proportion of contacts in schools and workplaces	0.32	[26, 27, 28]	
ϵ	Effectiveness of physical distancing	0.64	[25]	All
δ_C	Minimum closure duration period	30	[29]	
νL	Threshold to close the province	81	[30]	Niassa
		63		Cabo Delgado
		113		Nampula
		177		Zambézia
		113		Tete
		10		Manica
		42		Sofala
		27		Inhambane
		29		Gaza
		723		Maputo
		1871		Maputo City

each province, employing the `.evaluate()` function, which is also implemented in the Python SALib library by Herman and Usher [36]. After running each submodel, we performed sensitivity analysis using the `.analyze_sobol()` function from the same library.

The sensitivity analysis of the intervention thresholds reveals a clear relationship between the timing of policy activation and the resulting epidemic dynamics.

To assess the impact of the national threshold on epidemic progression, we simulated different values of νG, ranging from very restrictive to permissive. The sensitivity analysis of the intervention thresholds reveals a clear relationship between the timing of policy activation and the resulting epidemic dynamics. As shown in Table 3, lower national thresholds lead to substantial delays in the national epidemic peak. When a very restrictive threshold of active cases is adopted, the peak occurs at day 251, representing a delay of 98 days relative to the no-intervention scenario. In contrast, a more permissive threshold leads to a peak at day 198, corresponding to a delay of only 45 days. These results indicate that earlier activation of nationwide interventions significantly enhances their effectiveness in slowing epidemic growth.

Table 3: Variation of the national threshold νG.

Scenario	νG	National peak average (days)	Delay relative to baseline
Very restricted	1000	251	+98
Baseline	3249	235	+82
Moderate	5000	219	+66
Permissive	10000	198	+45

A similar pattern emerges in the analysis of provincial thresholds (νL). To illustrate this effect, we varied the provincial threshold for Manica, a province with a notably low baseline threshold. Table 4 summarizes the outcomes.

When the intervention threshold is low, the epidemic peak occurs at day 305, representing a delay of 162 days relative to the baseline scenario. As the threshold increases, the peak occurs progressively earlier, reaching at day 221. This reduction of more than 80 days highlights the strong influence of local decision thresholds on epidemic timing.

Table 4: Variation of the provincial threshold νL (example in Manica).

Scenario	νL	Peak date in Manica	Delay relative to baseline
Baseline (Lower)	10	305	+162
Moderate	50	287	+144
High	200	251	+108
Very high	500	221	+78

3 Results and Discussion

In addition to comparing centralized and decentralized intervention strategies during the first wave of COVID-19 infections in Mozambique, which was the focus of our previous work [37], the present study extends the analysis by examining the robustness of intervention outcomes under different policy and behavioral conditions. Specifically, we investigated how variations in physical distancing effectiveness, national intervention thresholds, and provincial thresholds influence epidemic dynamics. The simulation period covered 350 days, from March 22, 2020, to March 7, 2021, corresponding to the early phase of the pandemic when non-pharmaceutical interventions constituted the primary control strategy.

3.1 Effectiveness of Centralized and Decentralized Interventions

The comparison of intervention strategies reveals clear differences in their effectiveness. As illustrated in Fig. 2, decentralized interventions consistently delayed the epidemic peak more than centralized policies across all provinces. Additional delays ranged from 29 days in Niassa to 82 days in Manica, with a national average delay of approximately 37 days relative to centralized interventions.

These findings highlight the importance of spatial heterogeneity in epidemic dynamics. Mozambique exhibits substantial regional variation in population density, mobility patterns, and socioeconomic conditions. Provinces such as Maputo City and Maputo Province function as major economic and transportation hubs with high levels of daily mobility, while northern and central provinces such as Niassa or Manica are less connected and have lower population densities. In such settings, epidemic growth is unlikely to occur uniformly across the national territory. Locally triggered interventions allow authorities to respond earlier to regional increases in transmission, thereby interrupting infection chains before the epidemic spreads to other provinces.

In contrast, centralized strategies rely on national epidemiological thresholds that may delay intervention in provinces experiencing early outbreaks. When control measures are activated only after national case numbers exceed a predefined threshold, provinces with faster epidemic growth may already be well into the exponential phase of transmission. Similar patterns have been reported in spatial epidemic models showing that the timing and geographic targeting of interventions strongly influence epidemic trajectories in network-structured populations [38].

From a public health perspective, delaying the epidemic peak is particularly valuable in countries with limited healthcare resources. Mozambique's health system operates with constrained hospital capacity and limited intensive care infrastructure, particularly outside major urban centers. A delay of several weeks in the epidemic peak can provide critical time to mobilize additional resources, expand treatment capacity, and strengthen surveillance and testing systems.

3.2 Spatial Heterogeneity in Epidemic Burden

The analysis of cumulative infections (Table 5) shows that decentralized interventions also produced modest reductions in the overall epidemic burden, with provincial reductions ranging from 0.74% to 6.86%. Although these reductions are relatively small compared with the large delays observed in peak timing, they still represent meaningful improvements in epidemic control.

Importantly, the magnitude of these reductions varied across provinces. Less connected provinces such as Cabo Delgado, Niassa, and Gaza experienced greater benefits from decentralized interventions, whereas highly urbanized provinces such as Maputo City showed smaller differences between strategies. This pattern reflects the role of mobility networks in shaping epidemic diffusion. Highly connected regions tend to experience faster and more synchronized epidemic waves due to frequent population movement and dense contact networks. In contrast, regions with weaker connectivity often exhibit slower epidemic propagation, allowing localized interventions to interrupt transmission more effectively.

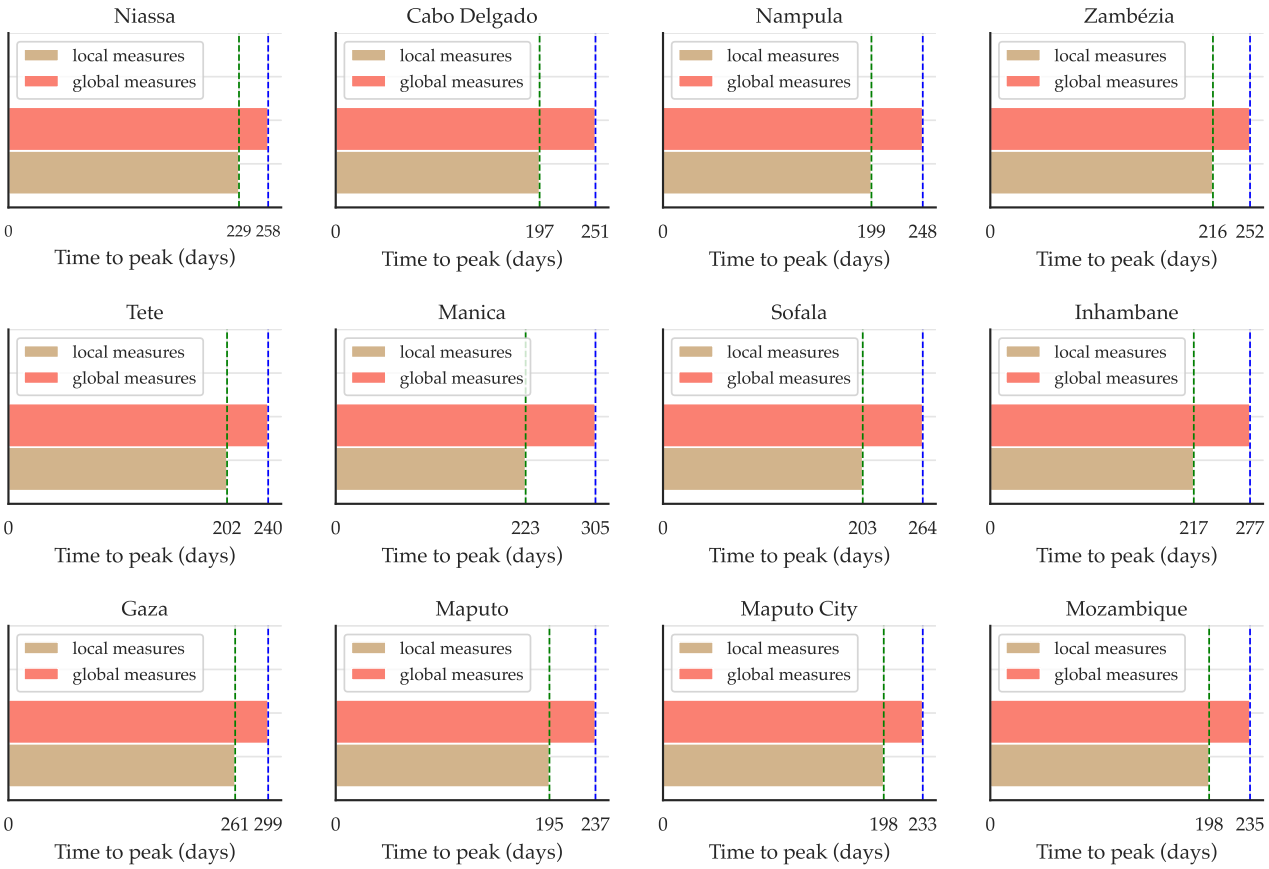

Figure 2: Comparison of epidemic peak timing between centralized and decentralized intervention scenarios across Mozambican provinces and at the national level. The green and blue dashed lines indicate the simulated peak days for the centralized and decentralized scenarios, respectively.

Table 5: Comparison of cumulative case counts between centralized and decentralized intervention scenarios across all Mozambican provinces and at the national level.

Province	Global Measures	Local Measures
Niassa	1990	1931
Cabo Delgado	2478	2308
Nampula	2458	2377
Zambézia	3871	3671
Tete	1693	1630
Manica	1703	1611
Sofala	2578	2443
Inhambane	1616	1604
Gaza	1572	1523
Maputo	9500	9419
Maputo City	21123	20807
Total	50582	49324

These findings are consistent with previous studies of spatial epidemic diffusion showing that heterogeneity in mobility and population distribution can generate substantial regional variation in epidemic timing and intensity [20, 39]. For countries such as Mozambique, where economic activity and population density are concentrated

in a small number of urban centers, these structural differences should be carefully considered when designing intervention strategies.

3.3 Impact of Behavioral Interventions

The sensitivity analysis of physical distancing effectiveness demonstrates a strong influence on epidemic dynamics. Across all provinces, higher effectiveness of distancing measures substantially delayed the infection peak (Fig. 3). In some provinces the delay exceeded 100 days when distancing effectiveness increased from 25% to 75%.

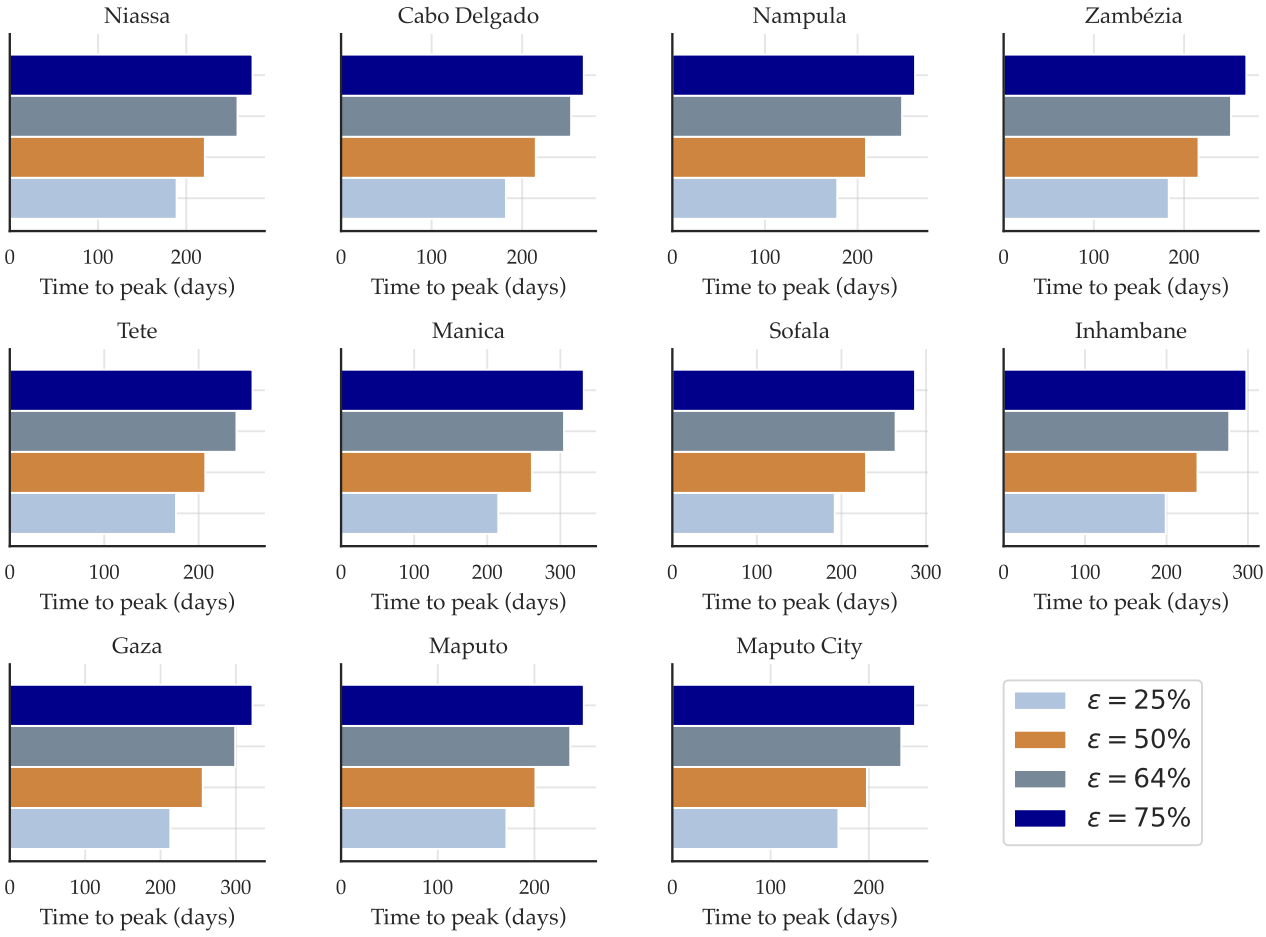

Figure 3: Time to peak infection by province under different values of physical distancing effectiveness.

However, the magnitude of this effect varied geographically. Provinces with lower population density and reduced mobility connectivity exhibited larger delays, whereas densely populated urban areas showed smaller improvements. This pattern reflects the fact that high-density environments sustain transmission even when behavioral interventions reduce contacts. Urban centers such as Maputo City therefore require stronger or complementary measures, including targeted mobility restrictions, testing, and isolation policies.

These results reinforce the critical role of behavioral interventions in epidemic mitigation, particularly in settings where pharmaceutical interventions such as vaccines are initially unavailable or limited. Previous modeling studies have similarly shown that physical distancing and mobility reductions can significantly alter epidemic trajectories and delay peak healthcare demand [40, 41, 42].

3.4 Importance of Early Intervention Thresholds

The threshold sensitivity analysis further highlights the importance of early policy activation. Lower thresholds for national and provincial interventions substantially delayed epidemic peaks. For example, a restrictive national threshold of $\nu G = 1000$ delayed the peak by nearly 100 days relative to the baseline scenario.

This finding reflects a fundamental principle of epidemic control: interventions implemented early in the epidemic trajectory are typically more effective than those introduced after widespread transmission has occurred. Once

the epidemic enters its exponential growth phase, delays in policy implementation can allow large numbers of secondary infections to occur before control measures take effect. The results therefore emphasize the importance of rapid surveillance and responsive policy triggers in controlling emerging infectious diseases.

3.5 Key Drivers of Epidemic Dynamics

The global sensitivity analysis based on Sobol indices (Fig. 4 and Fig. 5) confirms that the transmission rate is the most influential parameter governing the timing of epidemic peaks. This result is expected, as transmission intensity directly determines the speed at which infection spreads through the population.

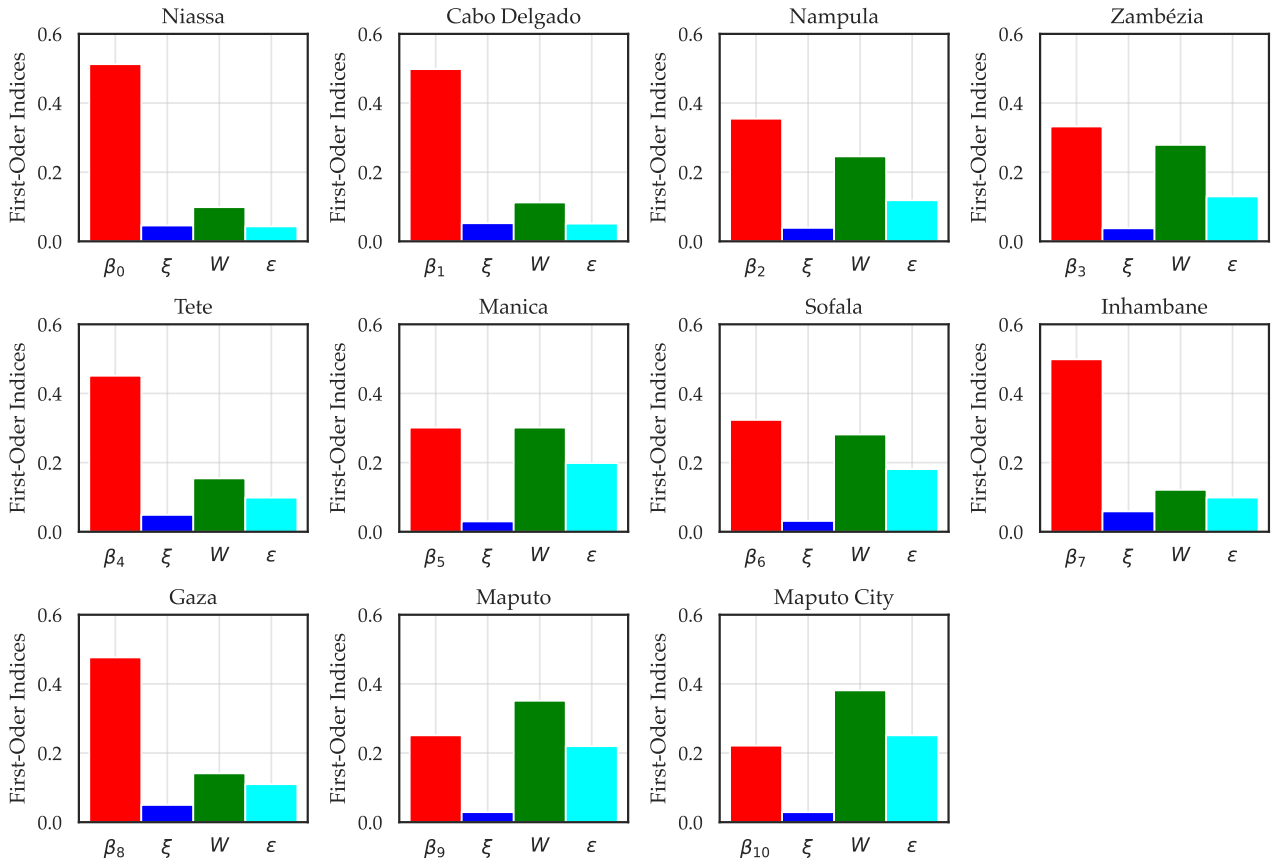

Figure 4: First-Order Indices (S_i) for the time of the infection peak.

Although individual effects of contact structure and distancing effectiveness appear smaller in the first-order analysis, the total-order indices reveal important interactions among parameters. In particular, the combination of high transmission potential and moderate intervention effectiveness can substantially alter epidemic trajectories. These interactions highlight the importance of considering both epidemiological parameters and behavioral responses when evaluating intervention strategies.

Overall, the results underscore the importance of mobility-aware, spatially explicit epidemic models for understanding disease dynamics in geographically diverse countries. By incorporating regional heterogeneity in population structure, mobility, and intervention responses, such models can provide valuable insights for designing adaptive public health policies in resource-limited settings.

4 Conclusion

This study investigated the impact of centralized and decentralized COVID-19 intervention strategies in Mozambique using a stochastic metapopulation SEIAHRD model that incorporates interprovincial mobility and heterogeneous contact patterns. By explicitly accounting for spatial structure and population movement between provinces, the model provides a realistic framework for evaluating how policy coordination influences epidemic dynamics in geographically diverse and resource-constrained settings.

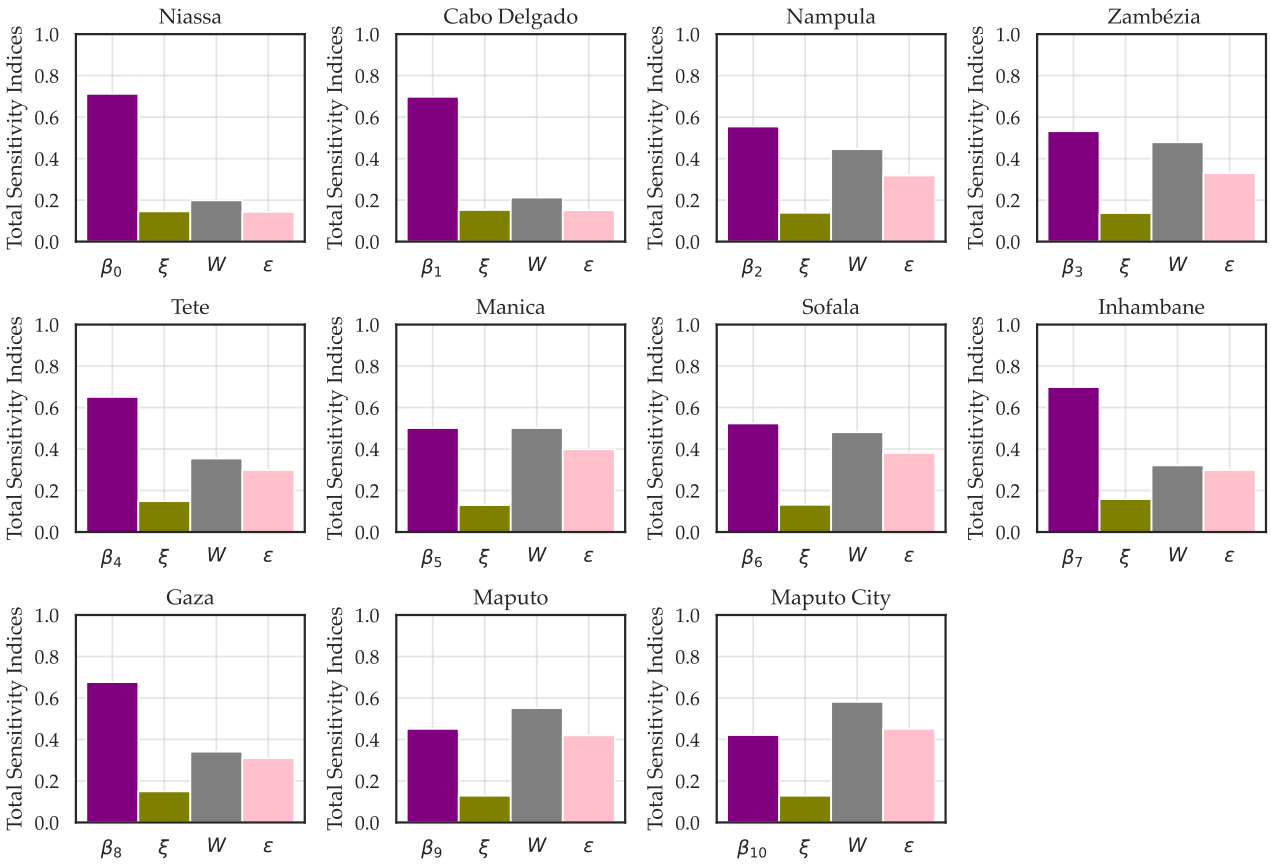

Figure 5: Total Sensitivity Indices (S_{T_i}) for the time of the infection peak.

Our results show that decentralized intervention strategies, triggered at the provincial level, consistently outperform centralized national responses in delaying epidemic peaks. Across provinces, decentralized policies delayed peak infections by 29 to 82 days, with an average national delay of approximately 37 days. These delays are particularly important in the Mozambican context, where health system capacity is limited and additional time can significantly improve preparedness, resource allocation, and hospital response during epidemic surges.

Although decentralized interventions produced only modest reductions in cumulative infections, the benefits varied substantially across provinces. Less connected and lower-density provinces experienced larger improvements, while highly urbanized and highly connected regions such as Maputo City showed smaller differences between strategies. This finding highlights the role of spatial heterogeneity and mobility patterns in shaping epidemic outcomes and suggests that uniform nationwide policies may not always be optimal in countries with diverse regional characteristics.

Sensitivity analyses further demonstrate that the effectiveness of behavioral interventions and the timing of policy activation are critical determinants of epidemic dynamics. Higher effectiveness of physical distancing measures and lower trigger thresholds for intervention substantially delay infection peaks. Global sensitivity analysis confirms that transmission intensity remains the dominant driver of epidemic timing, while interactions between contact patterns and intervention effectiveness can significantly amplify or mitigate policy impacts.

Taken together, these findings emphasize the importance of spatially adaptive and mobility-aware policy design in epidemic management. In the Mozambican context, decentralized intervention frameworks that allow provinces to respond rapidly to local transmission conditions may provide a more flexible and effective strategy than uniform national lockdowns. Such approaches can help balance epidemic control with socioeconomic considerations, particularly in settings where large segments of the population depend on informal economic activities.

Future research could extend this framework by incorporating additional real-world complexities, including age-structured contact patterns, vaccination dynamics, and behavioral adaptation over time. Integrating these factors into spatially explicit epidemic models will further improve the ability of policymakers to design targeted, evidence-based interventions for future public health emergencies.

Funding

This work was carried out under the COVID-19 Africa Rapid Grant Fund supported under the auspices of the Science Granting Councils Initiative in Sub-Saharan Africa (SGCI) and administered by South Africa's National Research Foundation (NRF) in collaboration with Canada's International Development Research Centre (IRDC), the Swedish International Development Cooperation Agency (Sida), South Africa's Department of Science and Innovation (DSI), the Fonds de Recherche du Québec (FRQ), the United Kingdom's Department of International Development (DFID), United Kingdom Research and Innovation (UKRI) though the Newton Fund, and the SGCI participating concils across 15 countries in sub-Saharan Africa to SAP (Reference Nr: COV19200617533083). SAP and PJ also was partially supported by Program UEM-SIDA 2017-2022 under the Subprogramme Nr 1.4.2: Capacity Building in Mathematics, Statistics and Its Applications.

References

[1] C. T. Bauch, J. O. Lloyd-Smith, M. P. Coffee, and A. P. Galvani, "Dynamically modeling SARS and other newly emerging respiratory illnesses: Past, present, and future," *Epidemiology*, vol. 16, no. 6, pp. 791–801, 2005. Available at: https://doi.org/10.1097/01.ede.0000181633.80269.4c

[2] I. M. Longini, A. Nizam, S. Xu, K. Ungchusak, W. Hanshaoworakul, D. A. T. Cummings, and M. E. Halloran, "Containing pandemic influenza at the source," *Science*, vol. 309, no. 5737, pp. 1083–1087, 2005. Available at: https://doi.org/10.1126/science.1115717

[3] A. Aleta, D. Martín-Corral, A. Pastore y Piontti, M. Ajelli, M. Litvinova, M. Chinazzi, N. E. Dean, M. E. Halloran, I. M. Longini Jr, S. Merler, A. Pentland, A. Vespignani, E. Moro, and Y. Moreno, "Modelling the impact of testing, contact tracing and household quarantine on second waves of COVID-19," *Nature Human Behaviour*, vol. 4, no. 9, pp. 964–971, 2020. Available at: https://doi.org/10.1038/s41562-020-0931-9

[4] S. Y. D. Valle, S. M. Mniszewski, and J. M. Hyman, *Modeling the Impact of Behavior Changes on the Spread of Pandemic Influenza*. New York, NY: Springer New York, 2013, pp. 59–77. Available at: https://doi.org/10.1007/978-1-4614-5474-8_4

[5] S. C. Anderson, A. M. Edwards, M. Yerlanov, N. Mulberry, J. E. Stockdale, S. A. Iyaniwura, R. C. Falcao, M. C. Otterstatter, M. A. Irvine, N. Z. Janjua, D. Coombs, and C. Colijn, "Quantifying the impact of COVID-19 control measures using a Bayesian model of physical distancing," *PLOS Computational Biology*, vol. 16, no. 12, pp. 1–15, 2020. Available at: https://doi.org/10.1371/journal.pcbi.1008274

[6] A. de Souza Melo, A. I. G. da Penha Sobral, M. L. M. Marinho, G. B. Duarte, A. A. Vieira, and M. F. F. Sobral, "The impact of social distancing on COVID-19 infections and deaths," *Tropical Diseases, Travel Medicine and Vaccines*, vol. 7, no. 1, p. 12, 2021. Available at: https://doi.org/10.1186/s40794-021-00137-3

[7] A. Brodeur, A. E. Clark, S. Flèche, and N. Powdthavee, "COVID-19, lockdowns and well-being: Evidence from Google trends," IZA Network @ LISER, IZA Discussion Papers 13204, 2020. Available at: https://ideas.repec.org/p/iza/izadps/dp13204.html

[8] N. Haider, A. Y. Osman, A. Gadzekpo, G. O. Akipede, D. Asogun, R. Ansumana, R. J. Lessells, P. Khan, M. M. A. Hamid, D. Yeboah-Manu, L. Mboera, E. H. Shayo, B. T. Mmbaga, M. Urassa, D. Musoke, N. Kapata, R. A. Ferrand, P.-C. Kapata, F. Stigler, T. Czypionka, A. Zumla, R. Kock, and D. McCoy, "Lockdown measures in response to COVID-19 in nine sub-Saharan African countries," *BMJ Global Health*, vol. 5, no. 10, p. e003319, 2020. Available at: https://doi.org/10.1136/bmjgh-2020-003319

[9] Conselho de Ministros, "Decreto presidencial nº 11/2020 de 30 de março: Declara o estado de emergência por razões de calamidade pública em todo o território nacional," Boletim da República, I Série, n. 61, p. 325-326, Maputo, Moçambique, 2020.

[10] Agência Lusa, "Covid-19. Medidas atempadas e apoios permitiram controlar epidemia em Moçambique, diz a OMS," 2020, Observador. Available at: https://observador.pt/2020/11/17/covid-19-medidas-atempadas-e-apoios-permitiram-controlar-epidemia-em-mocambique-diz-a-oms/

[11] L. E. G. Mboera, G. O. Akipede, A. Banerjee, L. E. Cuevas, T. Czypionka, M. Khan, R. Kock, D. McCoy, B. T. Mmbaga, G. Misinzo, E. H. Shayo, M. Sheel, C. Sindato, and M. Urassa, "Mitigating lockdown challenges in response to COVID-19 in Sub-Saharan Africa," *International Journal of Infectious Diseases*, vol. 96, pp. 308–310, 2020. Available at: https://doi.org/10.1016/j.ijid.2020.05.018

[12] D. M. Julião and P. C. C. Cambrão, "Effects of lockdown policies for COVID-19 in Mozambique: Reflecting on perceptions about the effects of pandemic containment policies," 2021, Collateral Global. Available at: https://collateralglobal.org/article/effects-of-lockdown-policies-for-covid-19-in-mozambique/

[13] G. Barletta, F. Castigo, E.-M. Egger, M. Keller, V. Salvucci, and F. Tarp, "The impact of COVID-19 on consumption poverty in Mozambique," *Journal of International Development*, vol. 34, no. 4, pp. 771–802, 2022. Available at: https://doi.org/10.1002/jid.3599

[14] R. Betho, M. Chelengo, S. Jones, M. Keller, I. H. Mussagy, D. van Seventer, and F. Tarp, "The macroeconomic impact of COVID-19 in Mozambique: A social accounting matrix approach," *Journal of International Development*, vol. 34, no. 4, pp. 823–860, 2022. Available at: https://doi.org/10.1002/jid.3601

[15] A. Sheikh, A. Sheikh, Z. Sheikh, and S. Dhami, "Reopening schools after the COVID-19 lockdown," *Journal of Global Health*, vol. 10, no. 1, p. 010376, 2020. Available at: https://doi.org/10.7189/jogh.10.010376

[16] R. O. Macalinao, J. C. Malaguit, and D. S. Lutero, "Agent-based modeling of COVID-19 transmission in philippine classrooms," *Frontiers in Applied Mathematics and Statistics*, vol. 8, p. 886082, 2022. Available at: https://doi.org/10.3389/fams.2022.886082

[17] Y. Li, E. A. Undurraga, and J. R. Zubizarreta, "Effectiveness of localized lockdowns in the COVID-19 pandemic," *American Journal of Epidemiology*, vol. 191, no. 5, pp. 812–824, 2022. Available at: https://doi.org/10.1093/aje/kwac008

[18] D. O'Sullivan, M. Gahegan, D. J. Exeter, and B. Adams, "Spatially explicit models for exploring COVID-19 lockdown strategies," *Transactions in GIS*, vol. 24, no. 4, pp. 967–1000, 2020. Available at: https://doi.org/10.1111/tgis.12660

[19] J. M. Amoedo, Y. Atrio-Lema, M. d. C. Sánchez-Carreira, and I. Neira, "The heterogeneous regional effect of mobility on Coronavirus spread," *The European Physical Journal Special Topics*, vol. 231, no. 18, pp. 3391–3402, 2022. Available at: https://doi.org/10.1140/epjs/s11734-022-00533-6

[20] P. Coletti, P. Libin, O. Petrof, L. Willem, S. Abrams, S. A. Herzog, C. Faes, E. Kuylen, J. Wambua, P. Beutels, and N. Hens, "A data-driven metapopulation model for the Belgian COVID-19 epidemic: assessing the impact of lockdown and exit strategies," *BMC Infectious Diseases*, vol. 21, no. 1, p. 503, 2021. Available at: https://doi.org/10.1186/s12879-021-06092-w

[21] Y. Li, L. Yu, X. Yang, T. Zhang, G. Sun, J. Lv, and Q.-H. Liu, "When mobility matters: How inter-regional travel shapes the effectiveness of local epidemic interventions," *Chaos, Solitons & Fractals*, vol. 200, p. 117001, 2025. Available at: https://doi.org/10.1016/j.chaos.2025.117001

[22] Q. Shao and D. Han, "Epidemic spreading in metapopulation networks with heterogeneous mobility rates," *Applied Mathematics and Computation*, vol. 412, p. 126559, 2022. Available at: https://doi.org/10.1016/j.amc.2021.126559

[23] P. Joaquim, D. Takahashi, and S. A. Pedro, "Understanding the role of human inter-provincial mobility on COVID-19 spread: a stochastic meta population model with time-dependent contact rates," *VETOR - Journal of Exact Sciences and Engineering*, vol. 35, no. 1, p. e18479, 2025. Available at: https://doi.org/10.63595/vetor.v35i1.18479

[24] P. Joaquim, D. Takahashi, and S. Pedro, "The role of interprovincial mobility in the dynamics of COVID-19 epidemic in Mozambique: Insights from a stochastic metapopulation model," in *Anais do Encontro Nacional de Modelagem Computacional e Encontro de Ciência e Tecnologia de Materiais*, Ilhéus, Brasil, 2024.

[25] V. A. Karatayev, M. Anand, and C. T. Bauch, "Local lockdowns outperform global lockdown on the far side of the COVID-19 epidemic curve," *Proceedings of the National Academy of Sciences*, vol. 117, no. 39, pp. 24 575–24 580, 2020. Available at: https://doi.org/10.1073/pnas.2014385117

[26] Instituto Nacional de Estatística, "Anuário estatístico 2020 – Moçambique," Instituto Nacional de Estatística, Maputo, Moçambique, Tech. Rep., 2021. Available at: https://ine.gov.mz/web/guest/d/anuario-2020_final

[27] O. Lisboa, "Covid-19 afecta empresas em Moçambique," 2021, RFI. Available at: https://www.rfi.fr/pt/mo%C3%A7ambique/20200410-covid-19-afecta-empresas-em-mo%C3%A7ambique

[28] Ministério da Ciência, Tecnologias e Ensino Superior, "Estatísticas e indicadores do ensino superior em Moçambique – 2020," Ministério de Ciência, Tecnologias e Ensino Superior, Maputo, Moçambique, Tech. Rep., 2023.

[29] A. Cassy, T. Marrufo, and S. Chicumbe, "COVID-19 em Moçambique: Relatório do 1º ano 2020-2021," Instituto Nacional de Saúde, Observatório Nacional de Saúde, Marracuene, Moçambique, Tech. Rep., 2021. Available at: https://ons.gov.mz/wp-content/uploads/2022/06/ONS-Relatorio-do-1o-Ano-da-COVID-19-Mocambique.pdf

[30] Ministério da Saúde de Moçambique, "COVID-19 boletins diários," Portal oficial do Ministério da Saúde, 2020.

[31] H. P. Duerr, S. O. Brockmann, I. Piechotowski, M. Schwehm, and M. Eichner, "Influenza pandemic intervention planning using InfluSim: pharmaceutical and non- pharmaceutical interventions," *BMC Infectious Diseases*, vol. 7, no. 1, p. 76, 2007. Available at: https://doi.org/10.1186/1471-2334-7-76

[32] D. H. Morris, F. W. Rossine, J. B. Plotkin, and S. A. Levin, "Optimal, near-optimal, and robust epidemic control," *Communications Physics*, vol. 4, no. 1, p. 78, 2021. Available at: https://doi.org/10.1038/s42005-021-00570-y

[33] A. Saltelli, P. Annoni, I. Azzini, F. Campolongo, M. Ratto, and S. Tarantola, "Variance based sensitivity analysis of model output. design and estimator for the total sensitivity index," *Computer Physics Communications*, vol. 181, no. 2, pp. 259–270, 2010. Available at: https://doi.org/10.1016/j.cpc.2009.09.018

[34] M. Lamboni, "Uncertainty quantification: a minimum variance unbiased (joint) estimator of the non-normalized Sobol' indices," *Statistical Papers*, vol. 61, no. 5, pp. 1939–1970, 2020. Available at: https://doi.org/10.1007/s00362-018-1010-4

[35] I. M. Sobol, "Global sensitivity indices for nonlinear mathematical models and their Monte Carlo estimates," *Mathematics and Computers in Simulation*, vol. 55, no. 1-3, pp. 271–280, 2001. Available at: https://doi.org/10.1016/S0378-4754(00)00270-6

[36] J. Herman and W. Usher, "SALib: An open-source Python library for sensitivity analysis," *Journal of Open Source Software*, vol. 2, no. 9, p. 97, 2017. Available at: https://doi.org/10.21105/joss.00097

[37] P. Joaquim, D. Takahashi, and S. Pedro, "Policy impacts of lockdown strategies in Mozambique: Insights from a mobility-based stochastic COVID-19 model," in *Anais do Encontro Nacional de Modelagem Computacional e Encontro de Ciência e Tecnologia de Materiais*, Montes Claros, Brasil, 2025.

[38] A. Topirceanu, M. Udrescu, and R. Marculescu, "Centralized and decentralized isolation strategies and their impact on the COVID-19 pandemic dynamics," *arXiv:2004.04222*, 2020. Available at: https://doi.org/10.48550/arXiv.2004.04222

[39] L. J. Thomas, P. Huang, F. Yin, X. I. Luo, Z. W. Almquist, J. R. Hipp, and C. T. Butts, "Spatial heterogeneity can lead to substantial local variations in COVID-19 timing and severity," *Proceedings of the National Academy of Sciences*, vol. 117, no. 39, pp. 24 180–24 187, 2020. Available at: https://doi.org/10.1073/pnas.2011656117

[40] S. Flaxman, S. Mishra, A. Gandy, H. J. T. Unwin, T. A. Mellan, H. Coupland, C. Whittaker, H. Zhu, T. Berah, J. W. Eaton, M. Monod, P. N. Perez-Guzman, N. Schmit, L. Cilloni, K. E. C. Ainslie, M. Baguelin, A. Boonyasiri, O. Boyd, L. Cattarino, L. V. Cooper, Z. Cucunubá, G. Cuomo-Dannenburg, A. Dighe, B. Djaafara, I. Dorigatti, S. L. van Elsland, R. G. FitzJohn, K. A. M. Gaythorpe, L. Geidelberg, N. C. Grassly, W. D. Green, T. Hallett, A. Hamlet, W. Hinsley, B. Jeffrey, E. Knock, D. J. Laydon, G. Nedjati-Gilani, P. Nouvellet, K. V. Parag, I. Siveroni, H. A. Thompson, R. Verity, E. Volz, C. E. Walters, H. Wang, Y. Wang, O. J. Watson, P. Winskill, X. Xi, P. G. T. Walker, A. C. Ghani, C. A. Donnelly, S. Riley, M. A. C. Vollmer, N. M. Ferguson, L. C. Okell, S. Bhatt, and Imperial College COVID-19 Response Team, "Estimating the effects of non-pharmaceutical interventions on COVID-19 in Europe," *Nature*, vol. 584, no. 7820, pp. 257–261, 2020. Available at: https://doi.org/10.1038/s41586-020-2405-7

[41] N. M. Ferguson, D. Laydon, G. Nedjati-Gilani, N. Imai, K. Ainslie, M. Baguelin, S. Bhatia, A. Boonyasiri, Z. Cucunuba Perez, G. Cuomo-Dannenburg, A. Dighe, I. Dorigatti, H. Fu, K. Gaythorpe, W. Green, A. Hamlet, W. Hinsley, L. C. Okell, S. van Elsland, H. Thompson, R. Verity, E. Volz, H. Wang, Y. Wang, P. G. T. Walker, C. Walters, P. Winskill, C. Whittaker, C. A. Donnelly, S. Riley, and A. Ghani, *Report 9: Impact of non-pharmaceutical interventions (NPIs) to reduce COVID19 mortality and healthcare demand*, 2020, Imperial College COVID-19 Response Team. Available at: http://hdl.handle.net/10044/1/77482

[42] J. M. Brauner, S. Mindermann, M. Sharma, D. Johnston, J. Salvatier, T. Gavenčiak, A. B. Stephenson, G. Leech, G. Altman, V. Mikulik, A. J. Norman, J. T. Monrad, T. Besiroglu, H. Ge, M. A. Hartwick, Y. W. Teh, L. Chindelevitch, Y. Gal, and J. Kulveit, "Inferring the effectiveness of government interventions against COVID-19," *Science*, vol. 371, no. 6531, p. eabd9338, 2021. Available at: https://doi.org/10.1126/science.abd9338